Evaluation of Hydrodynamic Effects of the sinus of Valsalva on the Native Aortic Valve

Inaugural-Dissertation

zur

Erlangung der Doktorwürde

der Universität zu Lübeck

-Aus der Sektion Medizin-

.

vorgelegt von

Junfeng Yan

aus VR China, Liaoning

Lübeck

2015

1. Berichterstatter/-in: Prof. Dr. med. H.-H. Sievers_____

2. Berichterstatter/-in: PD. Dr. M. Großherr_____

Tag der mündlichen Prüfung: _____21.01.2015_____ _____

Zum Druck genehmigt. Lübeck, den   _____21.01.2015_____

Abbreviations

$AVOA_1$	maximum opening area of aortic valves
$AVOA_2$	orifice area at the end of initial slow valve closing phase
decisec	decisecond
$\Delta AVOA_{1-2}$	differences of valve orifice area during initial slow valve closing phase
dia	diastolic
dp/dt	hydrodynamic pressure
ISSCT	initial slow systolic valve closing time
ISSCV	initial slow systolic valve closing velocity
LC	left coronary sinus
MVOA	maximal valve opening area
NC	non-coronary sinus
$piece_{t2-t1}$, pie_{t2-t1}	frames recorded in the initial slow valve closing phase
R, r	radius
RC	right coronary sinus
RVCT	rapid valve closing time
RVCV	rapid valve closing velocity
S	semi-perimeter
SCD	slow valve closing displacement
sec	second
SSCT	slow systolic closing time
sys	systolic
t_1	valve opening time up to the maximal opening orifice
t_2	time of ejection phase
TR	transceiver receiver
TVP	transvalvular pressure
V, Vol	volume
VOA	valve opening area
VOT	valve opening time
VOV	valve opening velocity

Content

1. Introduction

1.1 Functional Anatomy

The sinuses of Valsalva are defined as the pouches between the aortic wall and each of the semilunar cusps of the aortic valves at the origin of the ascending aorta [Fig1]. These lie behind the flaps of the semilunar valves. Three sinuses are named as the left, right and non-coronary sinus. In addition, the first two sinuses host the ostien of the coronary arteries. They reach proximally from the leaflets attachment to the sinotubular junction distally [20] and incorporated into the aortic root.

The sinuses of Valsalva have their walls predominantly made up of aortic ones, but the sinus walls are thinner than the aorta [7, 19, 31]. Histologically, the sinus wall basically consists of type I collagen in the lower section proximal to the leaflets attachment where the muscle fibers insert into the left ventricle. But the type I collagen fibers progressively lost their predominance in the upper section of the sinus, while the elastic fibers enhance their partial role in this part [Fig2] [20].

Hemodynamically, the systolic aortic streaming viscous blood functioned as an unsteady mainstream flow along with vortices that spin in the sinuses of Valsalva [16, 24]. In the late diastole, the aortic flow downtrends without variation in radial velocity, while the thin boundary layer of the mainstream travels next to the aortic wall, but distal to the sinuses. This sinus vortex has an equilibrium position along the midline, which is uniquely determined by assuming that a streamline separating from the upstream border of the sinus reattaches at the downstream border. The presence of such a strong vortex potentially generates a pressure distribution in the plane of the leaflets that can close the valve when the aortic flow is decelerating [25, 40].

Since Leonardo da Vinci first drew and showed the sinus of Valsalva in 1513 [Fig3], his study of its hemodynamic function in the closing mechanism of the aortic valves was just reviewed and realized in about 500 years [28]. But this topic aroused many field investigations to understand the exact details of the mechanism since years. Some results remain limited and somehow controversial. An annotation of the effects of the aortic sinuses in the motion characteristics of the aortic valve is not completed. Some studies simulated the tubular aortic root

anatomy with three sinuses in artificial materials and analyzed the physiological effects on the aortic leaflets. It is hypothesized that the aortic sinus may affect the motion characteristics of the aortic valve [6, 7, 28, 31, 34, 38, 40]. This study was designed to investigate the effects of the sinus of Valsalva on the motion characteristics of the native aortic valve.
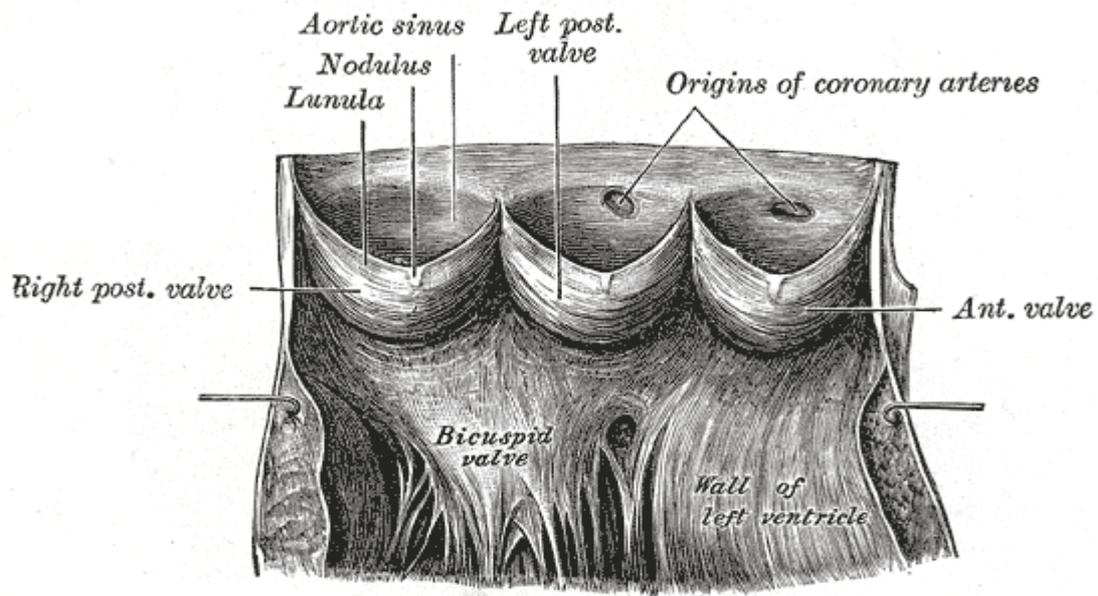
Fig. 1: Anatomy of the sinuses of Valsalva in axial section. (from Gray's Anatomy of the Human Body, Cor, FIG. 497)
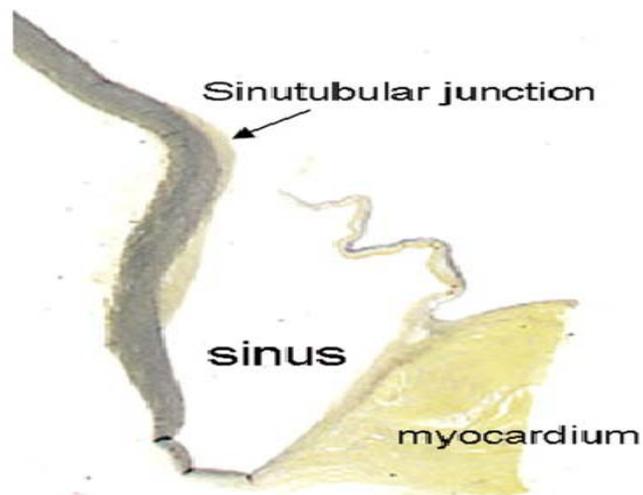

Fig. 2: Histological section (here right coronary sinus) shows the musculature in the depth of the sinus in elastic van Gieson stain.
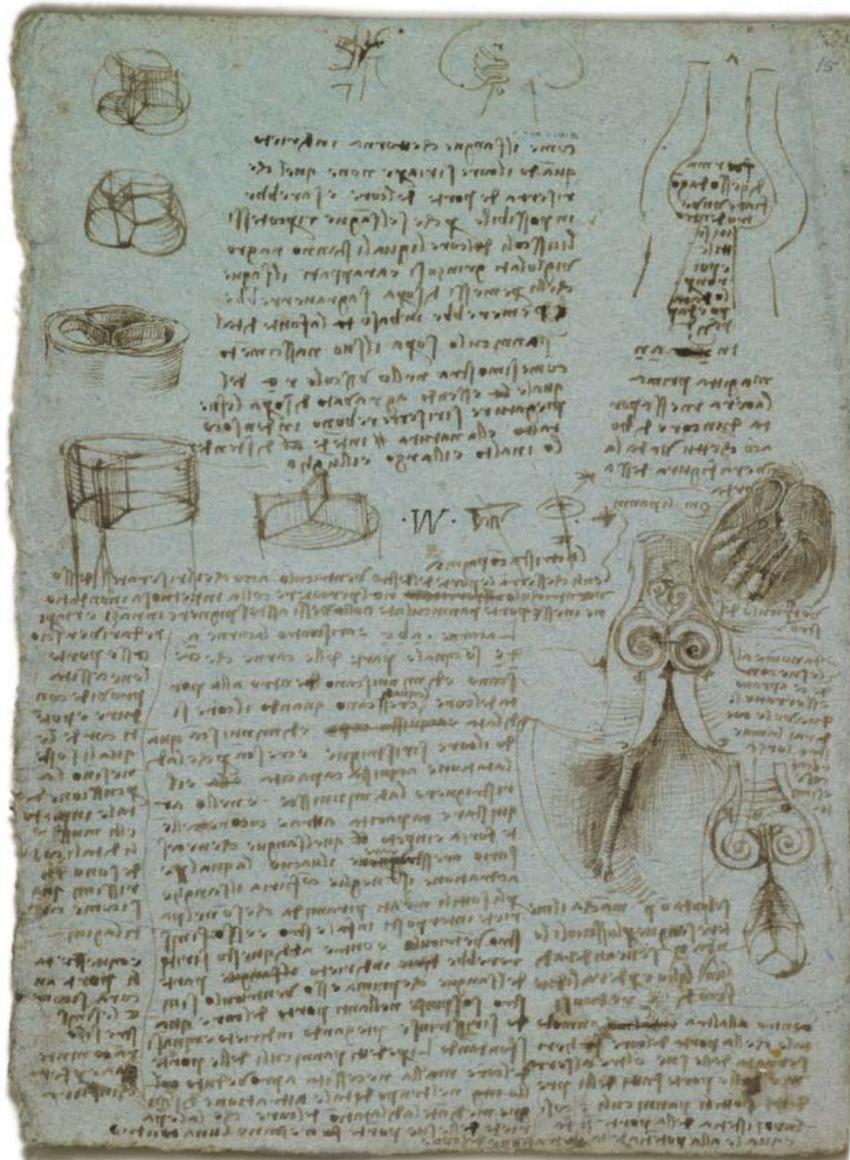
Fig. 3: In 1513, Leonardo da vinci first drew the aortic sinuses and a glass model to illustrate the hydrolytic mechanism. (RL19082 recto, ©The Royal Collection, Windsor Castle, England)

2. Materials and Methods

2.1 Aortic root model

Aortic roots were thoughtfully resected from pig hearts within 12 hours directly after the slaughter. The ascending aorta was cut circa 3 cm above the sinutubular junction, but under the ascending arch adjunction [Fig4-A].
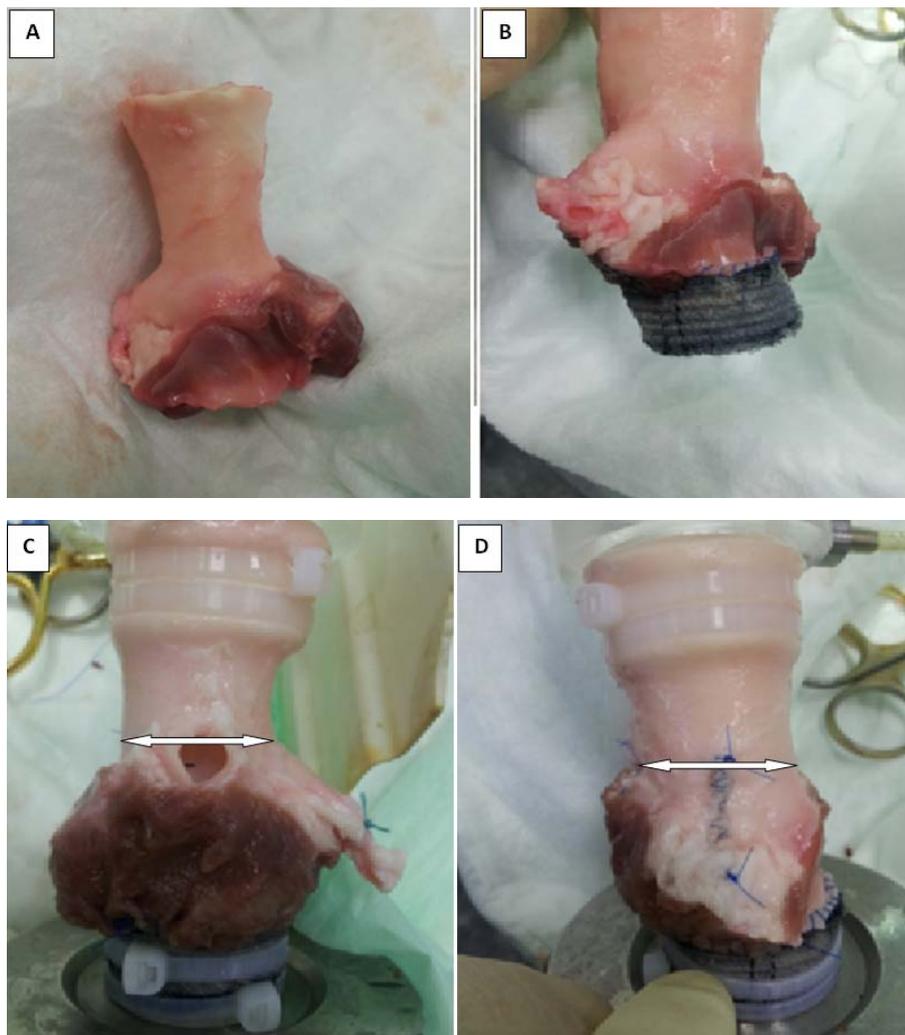
Fig. 4: Preparations of the aortic root model in the hydrodynamic test circuit [29]. A) carefully resecting the aortic root from porcine heart; B) suturing the aortic root into a Dacron tube section (Diameter: 24mm) for the consequent montage; C) cutting-off the sinuses of Valsalva with care of the integrity of the rest root structures; D) sewing-off the rest defect after the procedure C with the root dimension almost identically maintained (double-heads arrows)

Then, the left ventricular muscle and the anterior leaflet of mitral valve were removed for a subsequent suturing in a Dacron tube section with its dimension of 24 mm in diameter and 15 mm in height [Fig4-B]. This was mounted in the coming hydrodynamic test circuit. In doing so, approximate one centimeter tissue was left between the prosthesis tube and the aortic annulus. The two main trains of coronaries were tied up, respectively. After the first measurement, the three sinuses of the Valsalva were cut off and sewn up, while the geometric dimension of the aortic root and the aortal ascending portion was kept unchanged for the further investigation [Fig4-C&D].

2.2 Hydrodynamic test circuit

The aortic roots were investigated in an experimentally established pulse duplicator system [Fig.5] [29]. This provides the physiological flow conditions and simulates a stroke volume of 60ml with definite pressures of systolic 120mmHg and diastolic 80mmHg at a rate of 64 strokes per minute. The cycling liquid presenting predicted hydrodynamics consists of physiological saline solution. Herewith, the valves' functionality concerning such substantial characteristics as flow resistance and regurgitation can be examined in an approximately physiological circulation system.

The arterial preload is provided by the open reservoir with adjustable liquid height. The liquid arrives over two parallel arranged disk valves representing the mitral valves into a short-stroke diaphragm piston, which is propelled by one control disk adjusted to the natural volume curve of the heart. The drive of the machine is frequency variable and the different stroke volumes can be adjusted by the exchange of the control disk. The air chamber which is adjustable at the pump outlet simulates the elasticity of the left ventricle. The flow conditions of the left ventricular outflow tract are imitated by another chamber directly below the valvular level. The heart valves to study were mounted freestanding between two holders in a test space above. As seen in Fig. 5, a deflection chamber with inspection glass through which an optical observation and photographs with a camera for the documentation of valvular motions are possible, located above the valves holders. The arterial afterload system of the simulator is composed of three

elements: 1.) a height-adjustable liquid column providing a constant diastolic vessel pressure; 2.) an adjustable air chamber simulating typical aortal elasticity; and 3.) further element imitating the peripheral resistance. The overflow locates at the upper end of the column from which the liquid arrives back into the arterial reservoir.
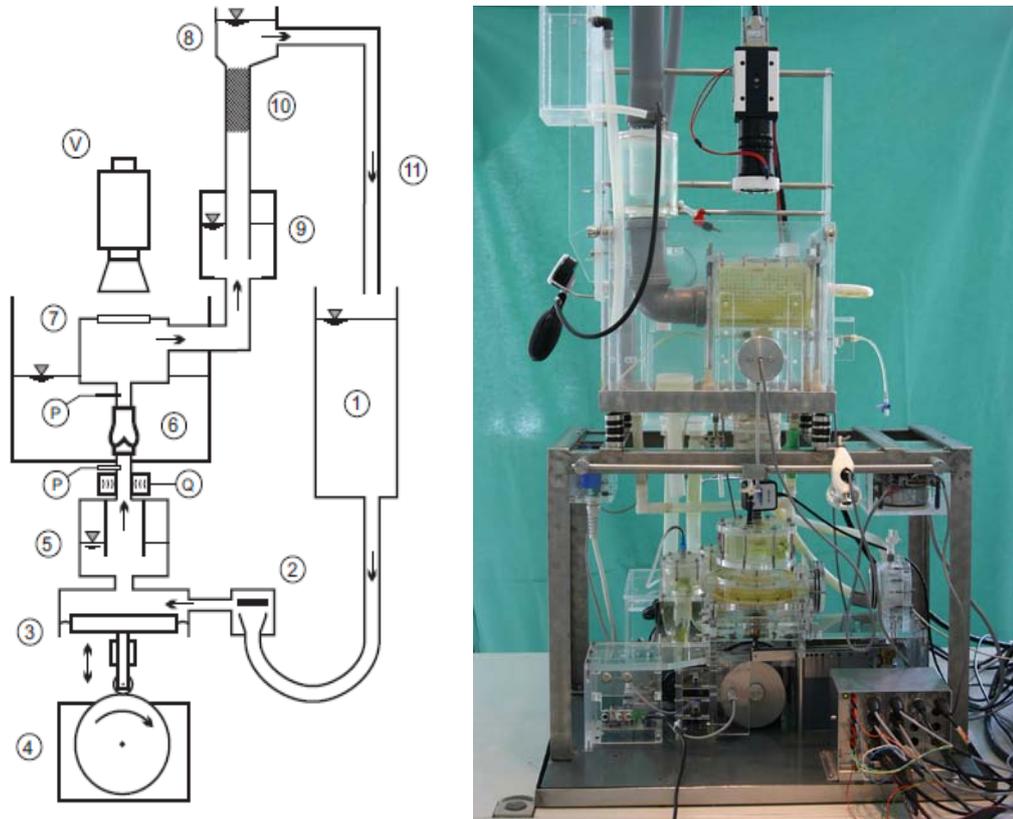
Fig. 5: Schematic depiction of hydrodynamic test circuit as a flow simulator [29] and finished model. 1.) atrial preload; 2.) mitral valve; 3.) pistons; 4.) electric power with control disk; 5.) ventricular compliance; 6.) testing space; 7.) deflection chamber with inspection glass; 8.) height variable liquid column; 9.) aortal compliance; 10.) peripheral resistance; 11.) return flow; P=pressure measurement; Q=volume measurement; V=video camera.

In course of hydrodynamic investigating, transvalvular pressure gradients and regurgitation volumes were recorded and accessed with the aid of Envec Ceracore M pressure transducers (Endress+ Hauser, Maulburg, Germany) and a TS410 ultrasonic flow meter (Transonic Systems Inc., Ithaca, NY, USA). The aortic valves' motion characteristics were taped and digitally measured by means of a motion scope HR-1000, a high-speed camera (Redlake Imaging Corp., Morgan Hill, CA, USA) which is adjustable over the aortic root model in a metal scaffold,

with a snapping frequency of 500 frames per minute. Video recording and volume flow measurements were simultaneously started and synchronized over trigger signals of the camera.

2.3 Evaluation of the recordings of the cusps motion

The leaflets motion was digitally recorded and converted into photo frames [Fig. 6]. These were analyzed by means of the ImageJ program (Rasband, W.S., ImageJ, U. S. National Institutes of Health, Bethesda, Maryland, USA, http://imagej.nih.gov/ij/, 1997-2014.). The orifice area of the aortic valves was calculated through following function (1.):

$$(1.)\ \text{Area}_{\text{Orifice}}\ (\text{cm}^2) = (\frac{\text{Montage base ring (cm)}}{\text{Length measurement (pixel)}})^2 \bullet \text{Area}_{\text{measurement}}\ (\text{pixel}^2)$$

* Montage base ring = 2.2 cm
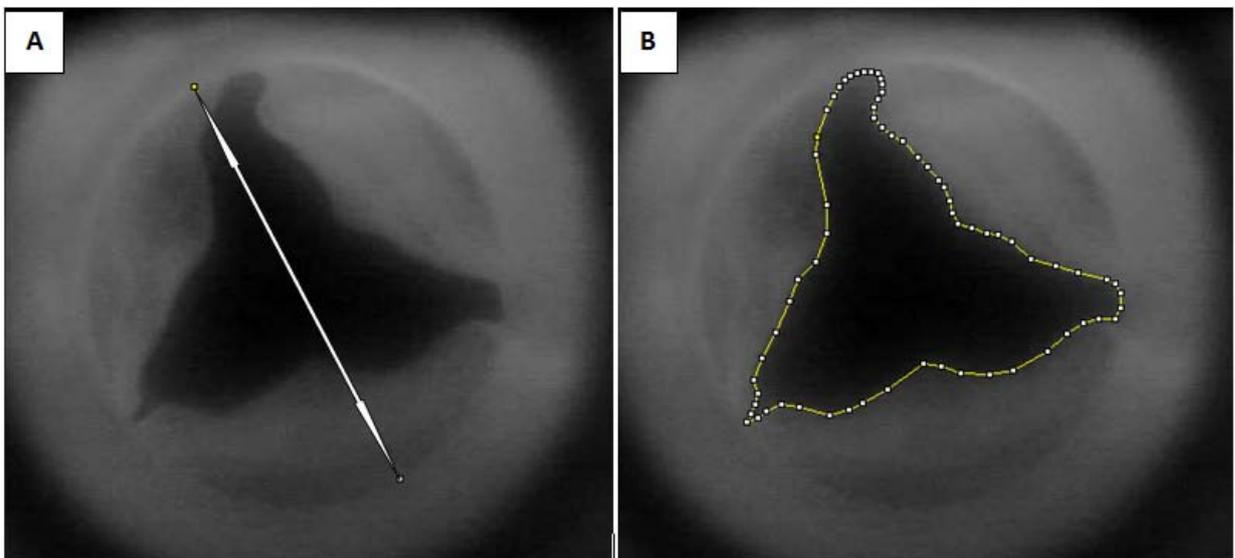
Fig. 6: This method utilizes highly sophisticated test equipment to provide an absolute measurement. A).The montage base ring is highlighted with white up-down-arrow and has fixed value of 2.2cm. B).The orifice area of the aortic valve is calculated by means of polygonal selection (yellow line) in ImageJ software.

2.3.1 Evaluation of the motion characteristics of the aortic valves' opening phase

The opening motion of the native aortic valve first recorded includes the distinct slow and rapid opening phases which were both together recorded and analyzed as a combined unit as valve opening motion in this study to refine the final analysis. These motion characteristics are the valve opening time (VOT), maximum opening area ($AVOA_1$) and valve opening velocity (VOV). This is calculated using following function (2.):

$$(2.) \quad VOV= \frac{AVOA1}{t1} \ (cm^2/sec)$$

2.3.2. Evaluation of the motion characteristics of the aortic valves' closing phase

2.3.2.1 Analysis of initial slow closing phase of the aortic valves

The early valve closing phase demonstrates its slow closing motion. The characteristics are digitally taped and analyzed as the initial slow systolic closing time (ISSCT), the initial slow systolic valve closing velocity (ISSCV), the orifice area at the end of this episode ($AVOA_2$) in this course and the slow valve closing displacement (SCD). Herewith, the ISSCV as curve slope was calculated in terms of angles' tangens in this phase by means of the AVOA difference between $AVOA_1$ and $AVOA_2$ divided by the SSCT (cm^2/decisec) or by the difference of photo sections recorded with the camera (cm^2/pic) in the same sense, respectively, equivalent to the tangens $\theta=\Delta AVOA_{1\text{-}2}/t_2\text{-}t_1$ (cm^2/decisec$_{t2\text{-}t1}$) or tangens $\theta=\Delta AVOA_{1\text{-}2}/pie_{t2\text{-}t1}$ (cm^2/pic), The parameters mentioned above could be executed by means of following functions (3.)(4.)(5.):

$$(3.) \ ISSCV = \frac{\Delta AVOA1-2}{t2-t1} \ (cm^2/sec)$$

$$(4.)\ \textbf{ISSCV} = \frac{\Delta AVOA1-2}{piecet2-t1}\ \textbf{(cm}^2\textbf{/pic)}$$

$$(5.)\ \textbf{SCD} = \frac{\Delta AVOA1-2}{AVOA1}\ \textbf{(\%)}$$

The end of this early slow systolic closing episode was remarked as the end of the ejection phase. This is characterized as no flow stream to evaluate in the flow curve registered by the TS410 ultrasonic flow meter.

2.3.2.2 Analysis of consequent rapid closing phase of the aortic valves

The late section of the closing motion of the native aortic valves was likewise analyzed. During this course, the rapid valve closing time (RVCT) and the rapid valve closing velocity (RVCV) are performed. Thereby, the rapid closing velocity was calculated as following (6.):

$$(6.)\ \ \textbf{RVCV} = \frac{AVOA2}{t3-t2}\ \textbf{(cm}^2\textbf{/sec)}$$

2.4 Evaluation and control of the transvalvular pressure gradient and flow volume characteristics

Pressures were measured by two capacitive pressure sensors Envec Ceracore M (Endress+Hauser, Maulburg, Germany). These were attached for the left ventricular pressure 4 cm below and for the aortic pressure 6 cm above the valve (Fig.5, P).This distance was selected to exclude possible falsifications of the pressure measurements caused by whirlpool formation behind the valve. The pressure sensors were thereby so calibrated that hydrostatic difference of pressure due to height difference became balanced. The sensors were preset by company to a measuring range from -20 to +160 mmHg, while the dissolution accounts to 0.02 mmHg. The volumetric flow rate through valves with an ultrasonic flow measuring instrument TS-410 (Transonic system Inc., Ithaca, NY, USA)

evaluated, whose sensor was directly installed underneath the valve (Fig.5, Q).This sensor measured volumetric flow rate by differences during the terms of the ultrasonic signal between the transmitter and receivers and can assess volumetric flow rates up to 20 L/min. The sensor works bidirectionally with a resolution of 2 ml/min.

The pressure and flow values were captured and recorded with a frequency by 500 values per second with the help of an analogue-digital converter. At least ten sequential heart cycles were recorded per measurement (for calculation of average values), with simultaneous video recording ever two heart cycles due to the limited bit map memory capacity of the camera. Herewith, several measurements were consecutively accomplished. The data evaluation took place in accordance with the international standard for testing of heart valves.
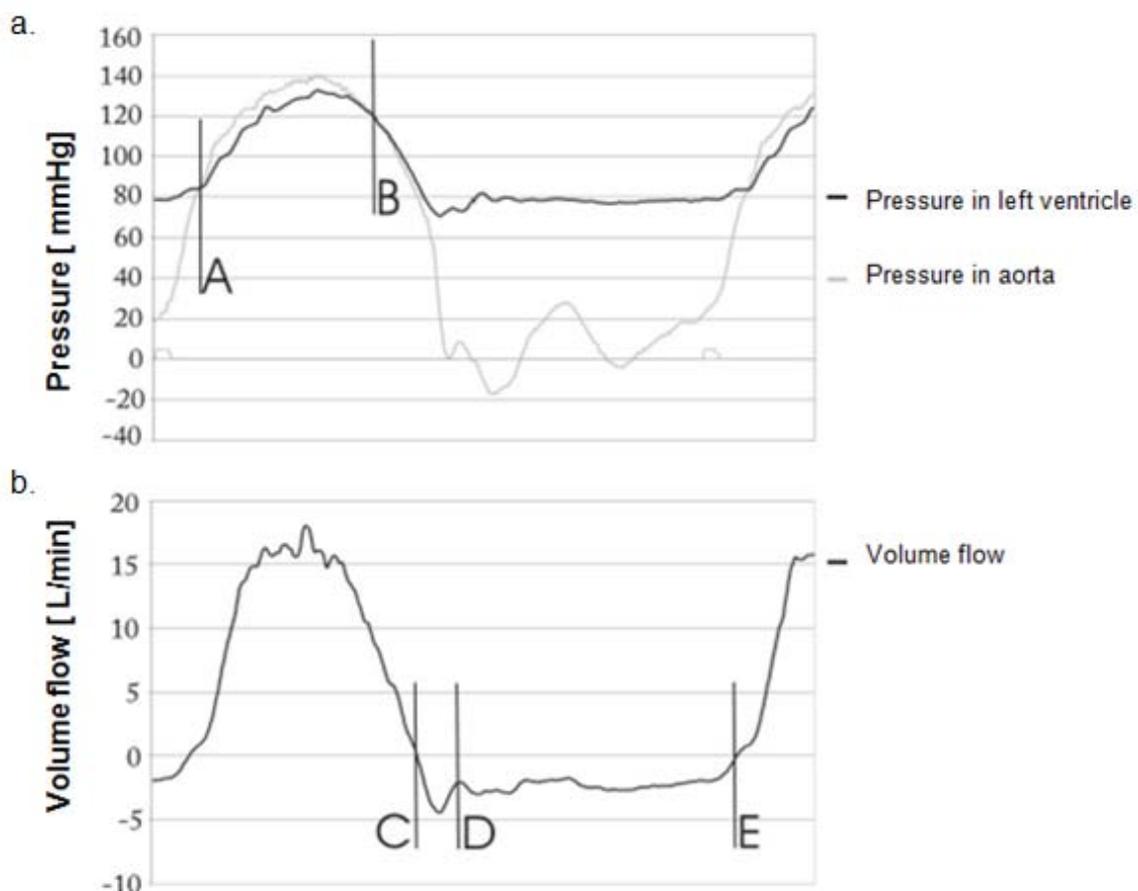

Fig. 7: Exemplary pressure and flow curves of one measured model in the study. a.: pressure curve. Equivalently, A=TVP mean (mmHg); B=TVP max (mmHg); b.: volume flow curve. C-D=V closure; D-E=V leakage.

The middle pressure gradient over the valve (TVP mean=average value of the positive pressure differences in the systole) [Fig.7a, A], the maximum pressure gradient (TVP max) [Fig.7a, B], the closing volumes (V close, which flows during the valve closing movement back into the left ventricle) [Fig.7b, C-D] and the leakage volume (V leak) [Fig.7b, E-D] in the diastole were determined as valve-specific parameters [Fig.7a+b].

Pressure gradients are indicated in mmHg. The volumes are indicated in ml/cycle. The valve motion and valvular opening area as well as possible deformation of leaflets with impairment of the coaptation were qualitatively evaluated from the video recordings.

2.5 Evaluation and control of the aortic root distensibility

Assessment of the distances between the respective sinus-root transitions in the interleaflet fibrous triangle at the commissural level is facilitated using ultrasonic micrometric transceiver receiver crystals (Sonometrics Corp. London, Ontario, Canada) to ensure the compliant status of all aortic root models before and after intentional sewing-off of the sinuses of the Valsalva. The crossing sectional areas at this affirmative level were calculated from the triangle defined by the distances between the corresponding crystals (A,B,C) at peak systolic and end diastolic pressures, respectively [Fig. 8] [18]. Thereby, the maximal and minimal areas were represented. The root distensibility was performed as the total percentage area alteration according to the value at the end diastole [13, 29, 30].

Three distances acquired from the measurement are performed as AB, BC and AC [Fig.8]. The semi-perimeter of the triangle is calculated as

$$(7.)\ s = \frac{AB+BC+AC}{2}$$

The area of the supposed circle is to achieve from the following formula:

$$\text{(8.) Radius} = \frac{s}{4*\sqrt{\frac{s*(s-AB)}{BC*AC}}*\sqrt{\frac{s*(s-BC)}{AB*AC}}*\sqrt{\frac{s*(s-AC)}{AB*BC}}}$$

$$\text{(9.) Area} = \pi r^2$$
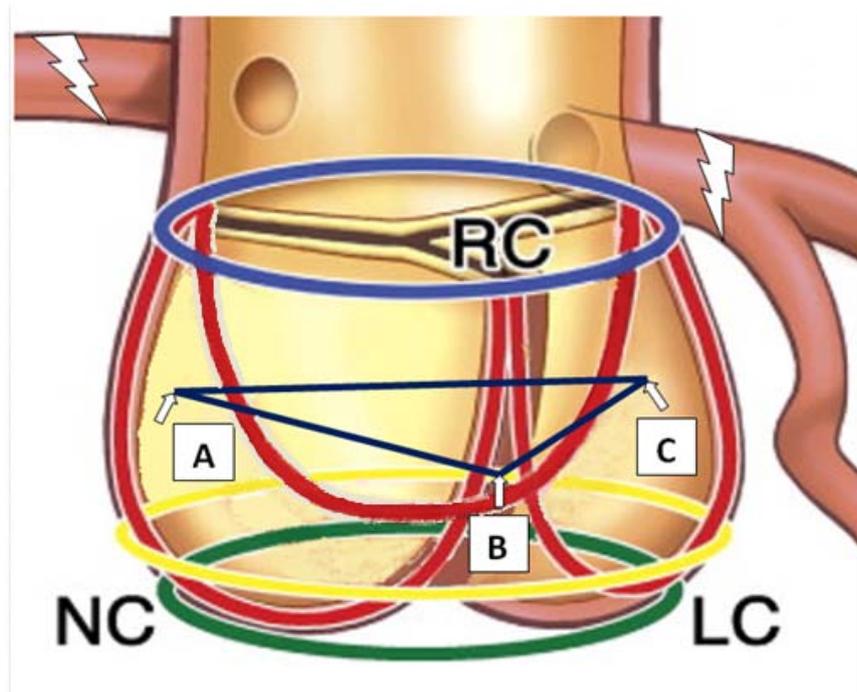
Fig. 8: Anatomical structures of the aortic root with schematic drawings of such important scaffolds as the crown-like sinuses of the Valsalva (red), the sinotubular junction at the commissural level (blue), the ventriculoaortic junction (yellow) and virtual annulus with the attachment of aortic leaflets (green) are given [14, 31, 35, 38]. Herewith, the locations of the ultrasonic micrometric TR-crystals are highlighted with white square arrows (A, B and C). In the study, a tying-up of the main trains of coronaries were targeted (lightning bolt). LC=left coronary sinus; RC=right coronary sinus; NC=non-coronary sinus.

As described above in Figure 8, the distances between the particular crystals (A, B, C) at the commissural level sewed outside on the sinus root junction is achieved to testify the compliance of all aortic root models before and after intentional sewing-off of the sinuses of the Valsalva. The crossing sectional areas were calculated at the peak systolic and the end diastolic pressures, respectively.

The root distensibility was performed as the total percentage area alteration according to the value at the end diastole.

$$\textbf{(10.) Root distensibility = Quotient} = \frac{Area\ sys - Area\ dia}{Area\ dia}\ \textbf{(\%)}$$

2.6 Statistic analysis

Statistical analysis was executed by means of SPSS Ver.16.0 (SPSS Inc. Released 2007. Chicago, SPSS Inc.). One-way ANOVA test and student t-test were used to compare the multiple series samples and to perform the significant differences. The valve motion characteristics were tested using the Chi-square analysis for the cross-table relationship. Pearson correlation test was undertaken to attest the reliable root distensibility. The data depicted in this study were expressed as mean ± the standard error of the mean. P values less than 0.05 were considered as significant.

3. Results

3.1 The motion characteristics of the aortic valves' opening phase

In the sinus group, the mean valve opening time up to maximal opening orifice area of the aortic valves accounts for 0.074 ± 0.004 seconds, the mean maximal opening area is 3.387 ± 0.126 cm^2, and the mean valve opening velocity in this course amounts to 46.29 ± 1.91 cm^2/sec, while the nonsinus group showed following characteristics as the mean valve opening time up to the maximal opening orifice of 0.072 ± 0.004 seconds ($p=0.792$, $t_{(16)}=0.269$), the mean maximal opening area of 3.001 ± 0.140 cm^2 ($p=0.057$, $t_{(16)}=2.053$), and the mean valve opening velocity of 41.76 ± 1.43 cm^2/sec ($p=0.076$, $t_{(16)}=1.896$) (see Tables 1, 2, 9, 10). There are no significant differences to evaluate in the characteristics of the valve opening motion between two groups.

	Sinus Valsalva	t_1 (VOT) (sec)	t_2 (sec) *	t_2-t_1 (ISSCT) (sec) *	t_3 (sec)	t_3-t_2 (RVCT) (sec) *
Mean ± SEM	yes	0.074 ± 0.004	0.338 ± 0.004	0.276 ± 0.004	0.409 ± 0.005	0.072 ± 0.005
	no	0.072 ± 0.004	0.316 ± 0.007	0.244 ± 0.006	0.406 ± 0.008	0.090 ± 0.005
p		$p=0.792$	$p=0.017$	$p=0.018$	$p=0.705$	$p=0.023$
$t_{(df)}$		$t_{(16)}=0.269$	$t_{(16)}=2.657$	$t_{(16)}=2.632$	$t_{(16)}=0.385$	$t_{(16)}=-2.514$
* $p < 0.05$; VOT=valve opening time; ISSCT=initial slow systolic valve closing time; RVCT=rapid valve closing time						

Tab. 1: Time registration for the hemodynamic motion of aortic valve in vitro HL-simulator. Herewith, three phases are presented as the valve opening time (VOT=t_1), initial slow systolic closing time (ISSCT=t_2-t_1) and rapid valve closing time (RVCT=t_3-t_2).

Error bars: +/- 1 SE
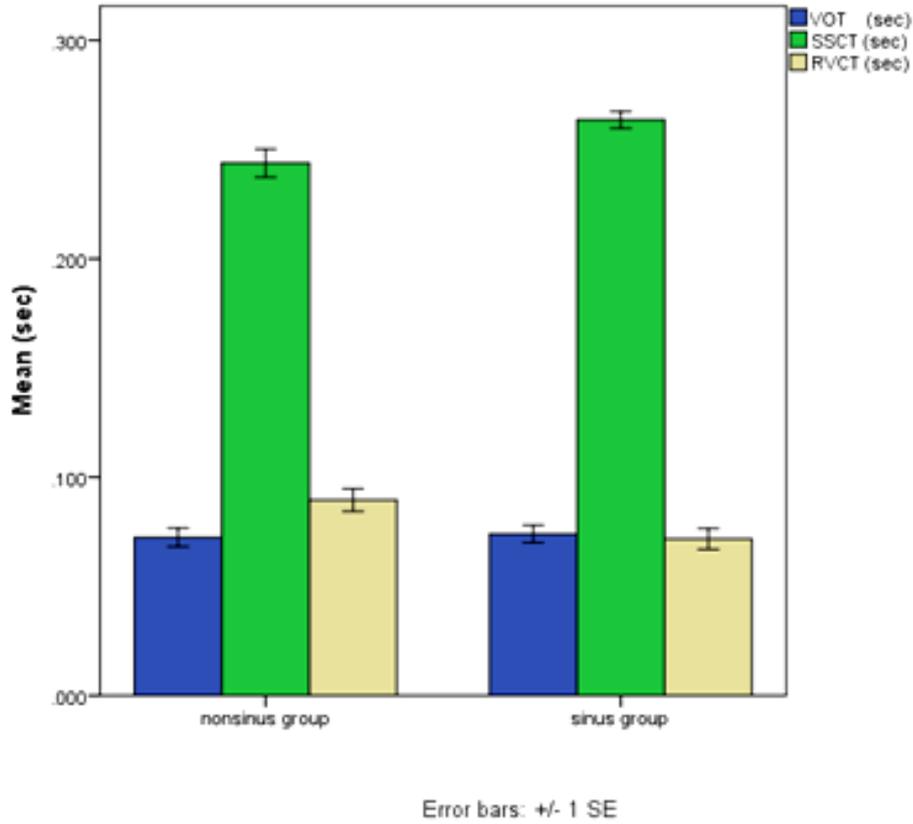
Fig. 9: Herewith, the three phase of the physiological motion of aortic valve was compared between sinus and nonsinus groups. The SSCT was significantly shortened in nonsinus group (p=0.018, $t_{(16)}$=2.632), while the RVCT significantly prolonged (p=0.023, $t_{(16)}$=-2.514).

	Sinus Valsava	$AVOA_1$ (cm^2)	$AVOA_1/t_1$ $(cm^2 \cdot s^{-1})$	$AVOA_2$	$\Delta AVOA_{1-2}$ (cm^2) *	SCD (%)
Mean ± SEM	yes	3.387± 0.126	46.29± 1.91	2.249± 0.150	1.137± 0.092	33.96± 8.87
	no	3.001± 0.140	41.76± 1.43	2.187± 0.143	0.813± 0.094	27.29± 13.35
p		p=0.057	p=0.076	p=0.769	p=0.026	p=0.007
$t_{(df)}$		$t_{(16)}$=2.053	$t_{(16)}$=1.896	$t_{(16)}$=0.299	$t_{(16)}$=2.455	$t_{(8)}$=3.621
* p < 0.05; AVOA=aortic valve opening area; ΔAVOA=difference of aortic valve opening area; SCD=slow closing valve displacement						

Tab. 2: Herewith, the nonsinus group showed generally a restricted maximal $AVOA_1$ (p=0.057, $t_{(16)}$=2.259),and decreased SCD (p=0.007, $t_{(8)}$=3.621), while the curve slope up to this maximal opening area was not significantly changed (p=0.076, $t_{(16)}$=1.896).
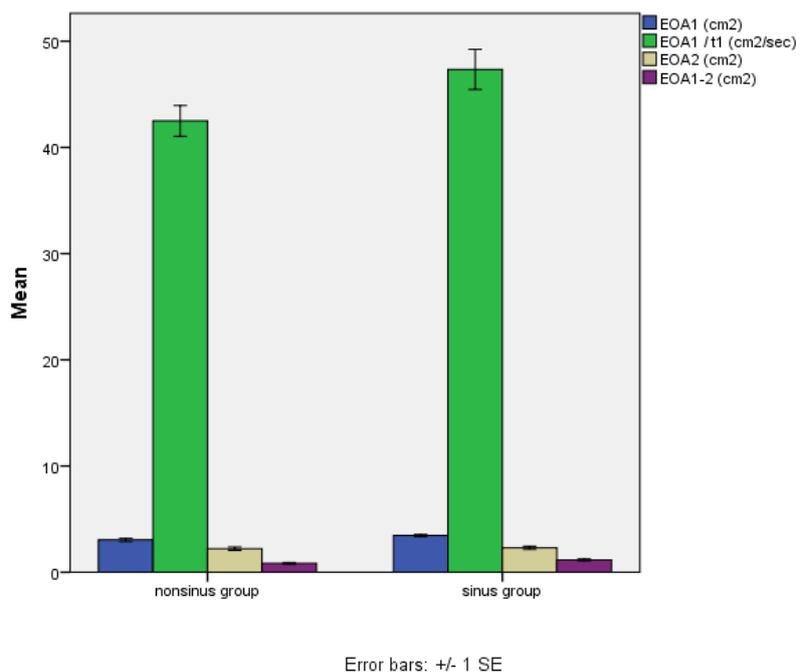
Fig. 10: The effective orifice areas were registered and analyzed in course of systolic and diastolic motion of aortic valve. Herewith, the differences of orifice areas and valve opening velocity between the both groups are not considered significant (p=0.057, $t_{(16)}$=2.053).

3.2 The motion characteristics of the aortic valves' closing phase

3.2.1 The motion characteristics of the slow valve closing phase

In the sinus group, the ISSCT accounts for 0.276± 0.004 seconds, the ISSCV is performed as tangens θ of the slope cure of the slow valve closing section as 0.431642± 0.035130 cm^2/ decisec or as 0.008633± 0.000703 cm^2/ pic, the slow valve closing displacement comes to 33.96± 8.87 % and the orifice area at the end of this phase is 2.249± 0.150 cm^2. But in the nonsinus group after intentional cutting-off of the sinuses, the ISSCT is 0.244± 0.006 seconds (p=0.018, $t_{(16)}$=2.632), the ISSCV accounts for 0.330917± 0.033158 cm^2/decisec or 0.006618± 0.000663 cm^2/pic (p=0.053, $t_{(16)}$=2.085), and the slow valve closing displacement presents 27.29± 13.35 % (p=0.007, $t_{(8)}$=3.621) (see Tables 1, 2, 3, 9, 10 and 11). The $AVOA_2$ comes to 2.187± 0.143 cm^2 (p=0.769, $t_{(16)}$= 0.299).

16

	Sinus Valsalva	Pieces $_{t2-t1}$ *	ISSCV=$\Delta AVOA_{1-2}$/pie$_{t2-t1}$ (cm^2/pic) *	ISSCV=$\Delta AVOA_{1-2}$/(t$_2$-t$_{1)}$ (cm^2/decisec) *
Mean ± SEM	yes	132± 2	0.008633± 0.000703	0.431642± 0.035130
	no	122± 4	0.006618± 0.000663	0.330917± 0.033158
p		p=0.018	p=0.053	p=0.053
t$_{(df)}$		t$_{(16)}$=2.632	t$_{(16)}$=2.085	t$_{(16)}$=2.085
* p< 0.05; ISSCV=initial slow systolic valve closing velocity; $\Delta AVOA$=difference of aortic valve opening area; pie$_{t2-t1}$=pieces of picture recorded during valve opening phase				

Tab. 3: Herewith, the ISSCV in sense of curve slope showed a relatively rigid progression in nonsinus group comparing to sinus group (p=0.053, t(16)=2.085).
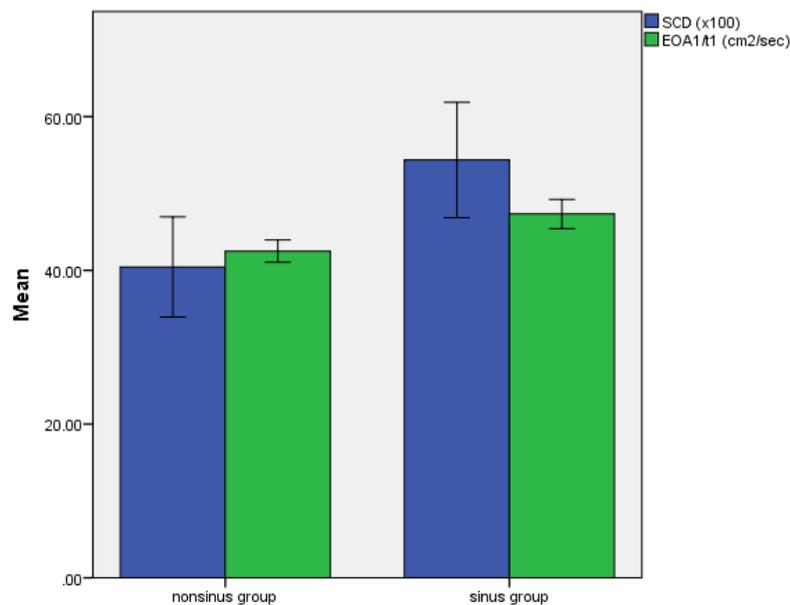
Error bars: +/- 1 SE

Fig. 11: The nonsinus group presented a non-significantly decreased SCD (p=0.151, t$_{(16)}$=1.507) and rarely changed valve opening velocity (p=0.076, t$_{(16)}$=1.896).

Herewith, the initial slow systolic valve closing time is significantly shortened after the intentional cutting-off of the sinuses of the Valsalva. Alike, the slow valve closing displacement decreased in the nonsinus group, while the initial slow systolic closing velocity is not essentially changed.

3.2.2 The motion characteristics of the rapid valve closing phase

The sinus group shows a rapid valve closing time of 0.072± 0.005 seconds and a rapid valve closing velocity of 31.88±2.26 cm^2/sec, while the nonsinus group presents a RVCT of 0.090± 0.005 seconds (p=0.023, $t_{(16)}$=-2.514)and a RVCV of 24.54±1.21 cm^2/sec (p=0.014, $t_{(16)}$=2.862) (see Tables 4 and 12). A prolangation of the rapid valve closing time and a decrease of the rapid valve closing velocity are significantly evaluated in the nonsinus group after intentional cutting-off of the sinuses of the Valsalva.

	Sinus Valsalva	t_3-t_2 (RVCT) (sec) *	AVOA$_2$(cm^2)	RVCV=AVOA$_2$/RVCT (cm^2/sec)
Mean ± SEM	yes	0.072± 0.005	2.249± 0.150	31.88±2.26
	no	0.090± 0.005	2.187± 0.143	24.54±1.21
p $t_{(df)}$		p=0.023, $t_{(16)}$=-2.514	p=0.769, $t_{(16)}$=0.299	p=0.014, $t_{(16)}$=2.862
* p < 0.05; RVCV=rapid valve closing velocity; RVCT=rapid valve closing time; AVOA=aortic valve opening area; SCD=slow closing displacement				

Tab. 4: A significant decrease of RVCV in the nonsinus group is assessed (p=0.014, $t_{(16)}$=2.862).

3.3 Transvalvular pressure gradient and regurgitation volume

In the sinus group, the peak and mean transvalvular pressures (TVP peak and mean) amount to 8.46± 0.77 mmHg and 2.96± 0.10 mmHg, respectively; the regurgitation volumes such as stroke, close and leak volumes (Vol stroke, close and leak) come to 70.00± 8.43 ml, -6.57± 0.65ml and -0.66± 0.11ml; the hydrodynamic pressure (dp/dt max) account for 432.56± 22.13 mmgHg/sec. While the nonsinus models show such comparable parameters as the TVP peak/mean of 9.56± 0.98 /3.39± 0.32 mmHg (for TVP peak: p=0.198, $t_{(11)}$=-1.370; for TVP mean: p=0.393, $t_{(11)}$=-0.889), the Volumes stroke/close/leak of 64.48± 0.98/ -7.45± 0.83/ -0.72± 0.14 ml (for stroke volume: p=0.561, $t_{(11)}$=0.599; for close volume: p=0.412,

$t_{(11)}$=0.853; for leakage volume: p=0.724, $t_{(11)}$=0.362), respectively, and the hydrodynamic pressure of 464.68± 18.85 mmHg/sec (p=0.302, $t_{(11)}$=-1.084). These hydrodynamic parameters are not significantly different in both groups (p > 0.05) (see Table 5).

	Sinus group	Nonsinus group	p ; $t_{(df)}$
TVP mean (mmHg)	2.96± 0.10	3.39±0.32	p=0.198 ; $t_{(11)}$=-1.370
TVP peak (mmHg)	8.46± 0.77	9.56±0.98	p=0.393 ; $t_{(11)}$=-0.889
V stroke (ml)	70.00± 8.43	64.48±0.98	p=0.561 ; $t_{(11)}$=0.599
V close (ml)	-6.57± 0.65	-7.45±0.83	p=0.412 ; $t_{(11)}$=0.853
V leak (ml)	-0.66± 0.11	-0.72±0.14	p=0.724 ; $t_{(11)}$=0.362

Tab. 5: Herewith, the physiologically interesting parameters registered in the opening and closing course were represented to enhance the hemodynamic changes after cutting-off of the sinus of Valsalva. Anyway, the nonsinus group showed a relatively distinct rigid character (TVP peak/mean and V stroke/close).

3.4 The distensibility of the aortic root before and after the manipulation of the sinuses of Valsalva

Three random sample pairs were realized in this method. The three sample values achieved from the group with the intact sinuses of the Valsalva are 0.357, 0.362 and 0.312, while the applicable values from the group after the intentional sewing-off of the sinuses are 0.358, 0.376 and 0.300 (see Tables 6 and 7). A Pearson product-moment correlation coefficient was computed to assess the relationship between values of both groups. There was a correlation to evaluate (r=0.990, n=3, p=0.045) (see Table 8). The root distensibility maintained unchanged after the manipulation.

pairs		phase	AB	BC	AC	S (mm)	r (mm)	Area (cm²)
1	Sinus	systole	35.924	32.570	32.570	50.532	19.5221164	11.9730189
		diastole	30.036	28.818	28.123	43.489	16.758034	8.82258817
	Nons inus	systole	34.632	31.477	31.179	48.644	19.2964959	11.0995063
		diastole	29.614	28.173	28.173	42.980	16.5577858	8.61299895
2	Sinus	systole	29.738	31.203	31.129	46.035	17.7310708	9.87688049
		diastole	26.384	26.334	26.235	39.477	15.1946377	7.25321535
	Nons inus	systole	26.782	27.750	29.167	41.850	16.9866948	8.18248736
		diastole	25.241	24.123	25.787	37.576	14.4788734	6.5859649
3	Sinus	systole	32.595	30.607	29.638	46.420	17.9121006	10.079591
		diastole	28.793	26.483	25.564	40.420	15.6226725	7.66761911
	Nons inus	systole	30.806	30.408	29.439	45.327	17.4553673	9.57211382
		diastole	27.526	26.433	25.464	39.712	15.3084962	7.36232415

Tab. 6: The distances were quantified by means of the three ultrasonic micrometric transceiver receiver crystals sewed outside in the fibrous interleaflet triangle at the commissural level. The values were obtained at the peak systolic and the end diastolic phase. (Details see 2.5 Evaluation and control of aortic root distensibility)

	Sinus Valsalva	Systole radius at ridge (mm)	Diastole radius at ridge (mm)	Quotient (R_{sys}/R_{dia})	Quotient $(A_{sys}-A_{dia})/A_{dia}$	Quotient $[(R_{sin}-R_{dia})/R_{dia}]$
No1	yes	19.52211	16.75803	1.1649	0.35709	0.16494
	no	19.29649	16.55779	1.1654	0.35816	0.16540
No2	yes	17.73107	15.19464	1.1669	0.36172	0.16693
	no	16.98669	14.47887	1.1732	0.37641	0.17321
No3	yes	17.91210	15.62267	1.14655	0.31457	0.14655
	no	17.45536	15.30850	1.14024	0.30015	0.14024
R_{sys}=radius measured in systole; R_{dia}=radius measured in diastole;						
A_{sys}=Area calculated in systole; A_{dia}=area calculated in diastole						

Tab. 7: To make sure that the anatomic ridge size of aortic root remained hydrodynamically quantity-stable after cutting-off of aortic sinus, an ultrasonic measurement system is set up in 3 pairs of preparation model to facilitate this evaluation and the systolic, especially the diastolic radius at ridge level were given, which showed less alteration. The distensibility of the aortic root is kept.

Correlations			
		Sinus group **Root Distensibility**	**Nonsinus group** **Root Distensibility**
Sinus group **Root** **Distensibility**	Pearson Correlation	1	.990[*]
	Sig. (1-tailed)		.045
	Sum of Squares and Cross-products	.001	.002
	Covariance	.001	.001
	N	3	3
Nonsinus group **Root** **Distensibility**	Pearson Correlation	.990[*]	1
	Sig. (1-tailed)	.045	
	Sum of Squares and Cross-products	.002	.003
	Covariance	.001	.002
	N	3	3
*. Correlation is significant at the 0.05 level (1-tailed).			

Tab. 8: A Pearson product-moment correlation coefficient was computed to assess the relationship between root distensibility values of both sinus groups. There was a correlation to evaluate (r=0.990, n=3, p=0.045).

3.5 Comparison of the aortic valves motion curves in one cycle in both groups

The motion curve of the aortic valves was depicted by means of the valve opening areas (VOA) which were registered in one cycle in the test series. The calculated VOAs were listed and analyzed in one motion cycle. Details were described in the sections of 2.2 and 2.3. The motion course of the aortic valves was divided into 4 parts such as the early systolic slow opening episode, the late systolic opening episode, the initial slow systolic closing episode and late rapid valve closing episode. The first two episodes were regarded as one valve opening unit to facilitate the evaluation in this study. Exempli gratia, one valve motion curve is presented below [Fig.12].
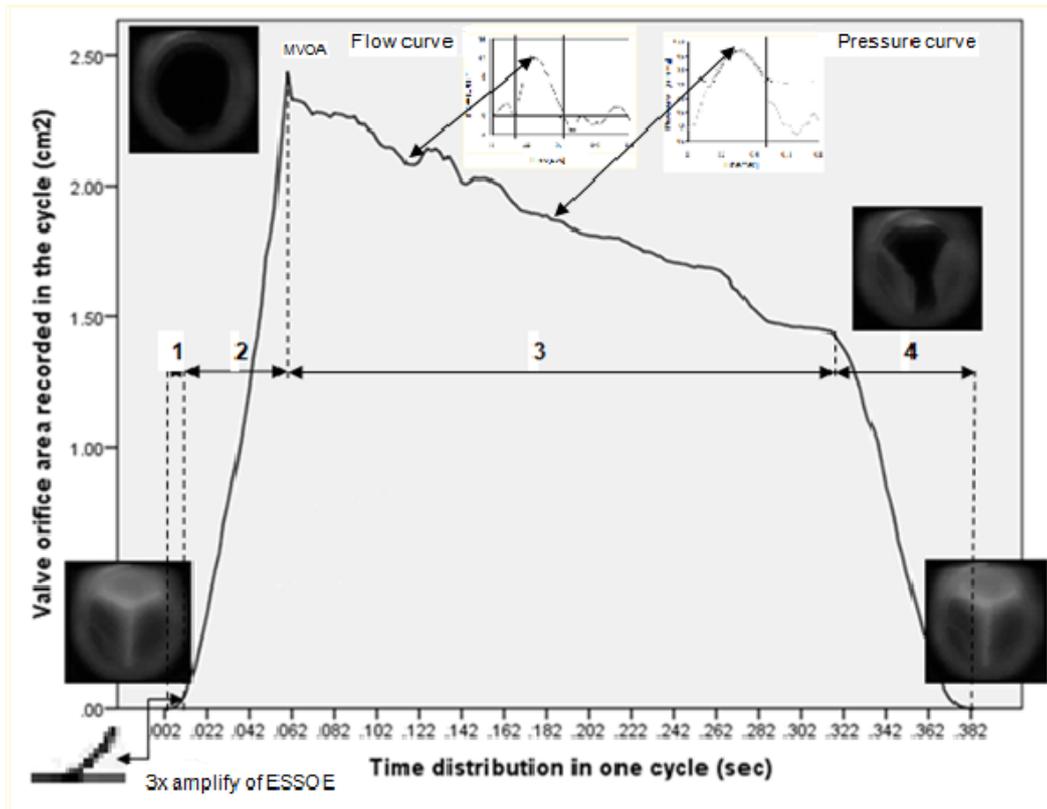
Fig.12: The graphics is depicted from the data assessed in a test sequence to elucidate the motion characteristics during the cardiac cycle. 1= early systolic slow valve opening episode; 2=late systolic rapid valve opening episode; 3= early systolic slow valve closing episode; 4= late systolic rapid valve closing episode. MVOA= maximal valve opening area

A comparison of the valve motion curves between two test models was carried out to highlight the distinct variations before and after the cutting-off of the aortic sinuses [Fig.13]. The both curve shapes show mostly equivalent properties despite of definite differences. Concluded from this, the motion behaviour of the aortic valves remained almost unchanged in the absence of the sinuses of Valsalva.
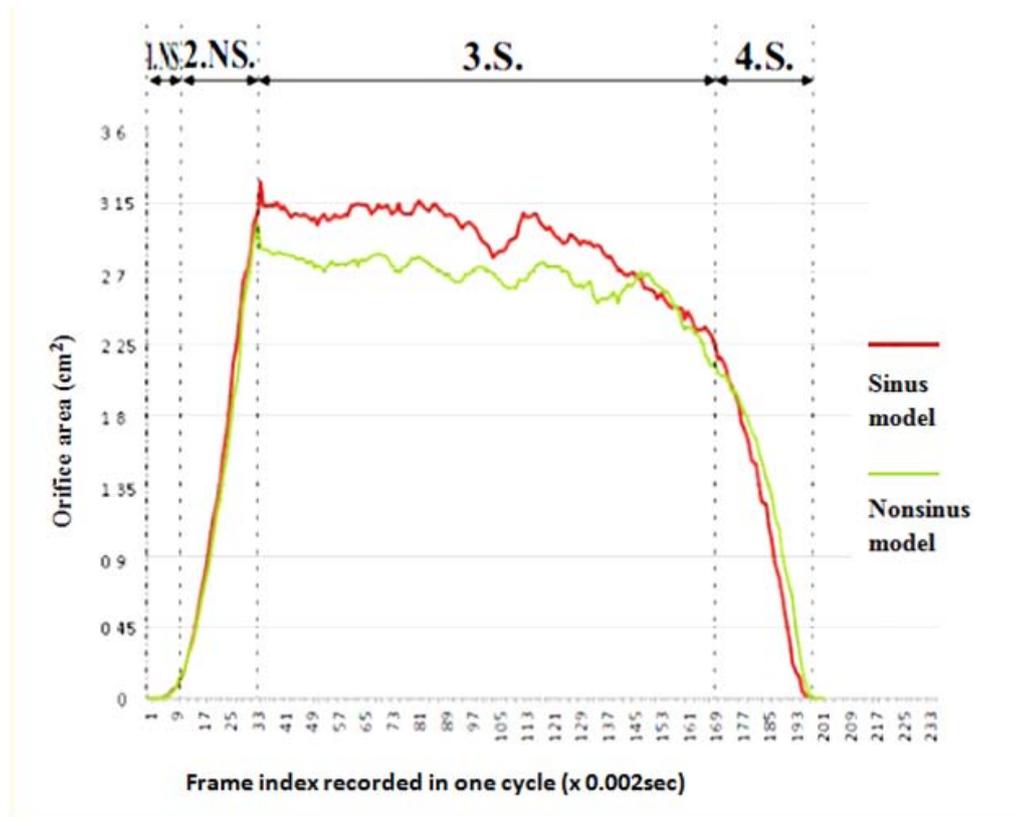
Fig. 13: To compare the mean valve motion behavior in one cycle in both groups. Herewith, the properties of valve opening areas were considered valve motion behavior. The valve opening phase (1+2) maintained unchanged (ns.), while initial slow and rapid valve closing phases (3+4) were somehow changed, albeit slightly. 1= early systolic slow valve opening episode; 2=late systolic rapid valve opening episode; 3= early systolic slow valve closing episode; 4= late systolic rapid valve closing episode. NS=not significant; S=significant.

4. Discussion

This study serves to investigate the effect of the sinuses of the Valsalva on the motion characteristics of native aortic valves in a flow simulator which provides familiar in vivo hemodynamic conditions to vivo conditions [11, 25, 26]. In order to understand function of the aortic sinuses in valve motion, we employed aortic root models derived from porcine hearts in which aortic root distensibility and diameter were maintained [13, 38].

Although Leonardo da Vinci first described the sinuses of the Valsalva in 1513; hitherto, the accurate function of the sinuses of Valsalva was not declared, let alone their effects on the motion characteristics of aortic valves. The experiment of model suggested by him was multiply reconstructed in different ways. The results remain controversial. Many studies have attempted to reproduce the tubular aortic root anatomy with artificial materials in order to assess the physiological effects of the aortic sinuses on the aortic leaflets in an equivalent simulator [6, 7, 8, 10, 14, 24, 26, 28, 29, 30, 38, 40]. Although, in these previous models, the flexibility of the aortic root was enhanced and narrowly preserved [6, 7, 8, 10, 24, 26, 29, 30, 38, 40], few were performed in a native aortic root. In order to gain a further insight into the physiological effects of the aortic sinuses on valvular motion in vivo, we performed this study in a native aortic root in a flow simulator with maintenance of aortic root geometry and distensibility. This was evaluated by consequent measurement of the distances of the particular sinus-root transitions in the interleaflet fibrous triangle at the commissural level to determine both diameter and cyclic alterations in sense of the aortic root distensibility. We enhanced and reiterated the unique effect of the sinuses of Valsalva on the valvular motion characteristics with unchanged root compliance.

As concluded from the investigations, opening motion characteristics of the leaflets such as valve opening time, maximal opening area and valve opening velocity remained relatively stable in the absence of the aortic sinuses (VOT $_{(mean)}$= 0.074±0.004 sec vs. 0.072±0.004 sec; AVOA$_{1(mean)}$= 3.387± 0.126 cm^2 vs. 3.001± 0.140 cm^2; AVOA$_1$/t$_{1(mean)}$= 46.29± 1.91cm^2/sec vs. 41.76± 1.43 cm^2/sec; p> 0.05). The hemodynamic parameters of the aortic valves remained unchanged as well

(TVP$_{peak/mean\ (mean)}$= 8.46± 0.77 / 2.96± 0.10 mmHg vs. 9.56± 0.98 / 3.39± 0.32 mmHg; Vol$_{stroke/close/leak\ (mean)}$= 70.00± 8.43 / -6.57± 0.65 / -0.66± 0.11ml vs. 64.48± 0.98/ -7.45± 0.83/-0.72± 0.14 ml; p> 0.05) [8]. Closing motion characteristics were but slightly impacted in the absence of sinuses: the initial slow systolic closing time was shortened (ISSCT $_{(mean)}$ = 0.276± 0.004 sec vs. 0.244± 0.006 sec, p< 0.05), the valve slow closing displacement diminished (SCD $_{(mean)}$ = 33.96± 8.87 % vs. 27.29± 13.35 %, p< 0.05), while a prolongation of the rapid closing time (RVCT $_{(mean)}$ = 0.072± 0.005 sec vs. 0.090± 0.005 sec, p< 0.05) was observed [Fig.12], while the initial slow systolic closing velocity (ISSCV $_{(mean)}$ = 0.431642± 0.035130 cm^2/ decisec vs. 0.330917± 0.033158 cm^2/decisec, p> 0.05), the valve opening area at the end of the ejection episode (AVOA$_2$ $_{(mean)}$ = 2.249± 0.150 cm^2 vs. 2.187± 0.143 cm^2, p> 0.05) and rapid valve closing velocity (RVCV $_{(mean)}$ = 31.88±2.26 cm^2/sec vs. 24.54±1.21 cm^2/sec, p> 0.05) remained unchanged. Thereby, some limitations of the preparation technique have been taken into account. As seen in Tables 6 and 10, aortic root radius of the second sample measured 17.73 mm during the systole and 15.19 mm during the diastole in the model with intact sinuses, compared to 16.99 mm and 14.48 mm, respectively after sinus removal. The maximal valve opening area of 2.529 cm^2 before the manipulation was reduced to 2.096 cm^2 after that. The reduction in the root radius may be responsible for the constrained maximal valve opening area despite of our efforts to limit this error.

Formally, the leaflet and the corresponding sinus both assemble a geometric cone unit extending constantly in the course of the pressure augmentation. It has been stated that the important component regulating valve leaflet curvature and motion is the original cone unit contour [6, 14, 16, 24]. However, our results indicate that the geometry of the sinuses of Valsalva may not be very relevant to the aortic valve opening and closing motion [40]. The leaflet motion is a continuous process with hydrodynamic properties during systole and diastole. The opening and closing motion features of valve leaflets suffer unbroken pulsatile flow stress, which is augmented by the cardiac contractile action. There are four main episodes of aortic valve leaflet motion to observe [Fig.13]: 1.) The early systolic slow opening motion episode of the aortic valve leaflets is induced by the isovolumetric contraction of the left ventricle. In this course, the pressure in the left ventricle

increases, the pressure difference across the valve decreases and the aortic leaflets initialize the onset of opening motion with resulting expansion of the aortic root, while no forward flow is assessable. 2.) The late systolic rapid opening motion begins immediately with the intraventricular pressure overcoming the intraaortic pressure. The blood is pumped out, opening the valves up to its maximal area. In a distensible aortic root, the diameter increases with the rising aortic pressure. In this way the cusp edge is held wrinkle-free. But the acceleration of the forward flow does not diminish until the peak of valve opening motion. 3.) After reaching the peak aperture, the leaflets begin to close in a constant slow motion. There are many opinions about the mechanisms of this early systolic slow closing motion. Some claim this is aroused by leaflet tension induced by the root expansion. The leaflet strain causes the formation of the aortic orifice triangular shape. Many assert that the vortex formation in the sinus pushes the leaflets inwards. However, it remains questionable, if such strong vortices are present at the beginning of the slow closing motion, as at this moment the leaflets reach their maximal aperture. The flow portion between leaflet and aortic wall or sinus dwindles in progress so far the stream flow keeps accelerating. This episode is actively supported by the pressure difference between the left ventricle and proximal aorta on the one hand, but on the other hand by the progressive passive distension of the aortic root. We found it feasible to use hydraulic Bernoulli principle to interpret our study results with total energy (E_{total}= KE+ PE) the same in both groups in the sense of incompressibility of the cycling saline solution in the flow simulator. This interpretation maintains the aortic root distensibility with an unvaried valve opening motion. Herewith, the transvalvular main flow velocity increases through a narrowed orifice with an increment of kinetic energy (KE $\propto$ V^2), as detected in this study [8]. Accordingly, the pressure energy decreases proportionally, decreasing burden on the aortic root. No need for a complete stretching of the root structures in the same model is understood. The slow valve displacement reduces as the closing velocity does. It is conceivable that the stable root distensibility determines the normal cups motion characteristics. Following the statement mentioned above, hydraulic Bernoulli principle can be reasonable for this phenomenon with an assumption of partial energy loss above the valve level. The forward flow continues to accelerate with ongoing amplitude expansion of the

proximal aorta until the maximum is reached, before the intraaortic or intraventricular pressure and aortic extension hit recorded highs. Then, the pressures and aortic extent decrease together with the regression of forward flow. The aortic valve leaflets closed gradually with fluttering properties over this course. The closing motion is partially assisted by the passive retractive action of the aortic root after its maximum width. This episode ends up to the moment the transvalvular forward flow ceases in the sense of the end of the ejection. Bernoulli principle distributes the effect of energy constancy all this way. 4.) The late rapid closing motion episode of the aortic valve leaflets is initialized by the backward axipetal blood stream. In addition to the further retractive force of the aortic root, the reflux supports this rapid valve closing act. The axipetal flow is directed not only into the sinuses of Valsalva but mostly towards the valve orifice. The intraventricular pressure decreases more than the intraaortic does. This reflux reaches its maximum with complete leaflet closure. The time of rapid leaflet closure which is partially, passively supported by the root contraction because of its flexibility, is prolonged. During all these episodes described above, a distensible aortic root is important for the smooth motion features of the valve leaflets. Though, many studies assert that the vortex formation in the sinuses reduces the stress on the aortic leaflets by means of preventing the leaflets from impacting the aortic wall in the systole and promoting a smoother valve closure [6, 7, 16, 24, 25, 29, 31, 38, 40]. Our observations and analysis lead us to believe, that while this vortex formation could affect motion characteristic, the effects are not crucial. Drawn from the study results, some hemodynamic parameters such as tranvalvular pressure gradient (TVP peak-mean), close and leakage volumes were changed [see Tab. 5], but not significantly [8]. Consequently, while reiterating that the study is concerned with investigation of the effects of sinus of Valsalva on the motion behaviors of native aortic valves, maximal reservation of aortic distensibility was pursued to exclude its impairing potential. This was ensured through maintenance of the whole native aortic root after much deliberation. Any other artificial materials imitating the aortal anatomical structures could more or less impress observation conditions to understand the essential hydrodynamics [8, 26]. Some groups claimed the isolation of aortic root compliance to evaluate the effects of sinus of Valsalva on the valvular hydrodynamics with synthetic materials, but

detailed analysis of physiological valves motion regarding distinct episodes was not essentially discussed [8, 26]. Moreover, to ensure the constancy of the aortic root compliance in the study, determination of the distances between each sinus-root transitions in the interleaflet fibrous triangle at the commissural level by means of ultrasonic micrometric transceiver receiver crystals (Sonometrics Corp. London, Ontario, Canada) ensued [see Tab.6 and 7] [new citation]. In this study, root distensibility was performed as the total percentage area alteration at peak systolic pressure according to the value at the end diastole. This method was evidence-based and experimentally established [11, 12, 25], while there are many modern techniques to assess aortic dimensions [4, 18, 31]. Anyhow, there is confusion in the interpretation of aortic valve area because of different diagnostic techniques. The differences depend mainly on the valve inflow shape and cross-sectional area of the ascending aorta. This study performed the geometric orifice area (GOA) which does not characterize the flow property.

In modern aortic valve sparing surgery, maintenance or regeneration of the sinuses facilitates restoration of the vortex formation in the sinuses and may favor normal leaflet motion as well as valve durability [6, 7, 10, 19, 24, 25, 29, 31, 38, 40]. This has been debated in such surgical armamentariums as Yacoub/ remodelling of aortic root and David/ reimplantation of aortic valves techniques since the early 1990s [2, 3, 5, 9, 11, 12, 13, 17, 19, 21, 22, 23, 32, 33, 34, 36, 37, 39, 41]. These procedures perform the replacement of the sinuses of Valsalva with a synthetic graft within which the cusps are resuspended. However, root replacement with a synthetic graft may result in an alteration of valve behaviour in terms of cusps coaptation and stress distribution which may lead to the failure of the correction purpose [5, 29, 30, 34]. Many studies were carried out to answer this question and found both techniques capable to restore aortic valve coaptation and to reduce stresses induced by the initial root dilatation [5, 13, 29, 30, 34]. Nonetheless, both techniques lead to altered leaflet kinematics. This is relatively more often observed in the David methods, especially with valve reimplantation in a cylindrical Dacron graft [1, 5, 9, 13, 15, 17, 27, 36, 39]. Compared to the native aortic root, the original David method with tubular graft performs no equivalent sinuses and restricts root compliance. The determinating factor of varied leaflet kinematics observed with this method is not ascertainable. On the other hand,

while the Yacoub technique presents better applicability and superiority of the maintenance of the root distensibility to reduce the alteration of the valve motion characteristics, entailing risks of delayed root redilatation for which David method shows its predominance [5, 13, 21, 22, 27, 34, 39]. This phenomenon may support the role of retained distensibility of the aortic root in smooth leaflet motion. To eliminate some of the disadvantages of different techniques and reconstruct a normal root anatomy, the Valsalva graft was introduced. It was mostly integrated into the aortic root modified as per David procedure. The initial results appear comparable to Yacoub's procedure with respect to valve motion performance [8]. Herewith, the sinuses are so restored that they are not separate as seen in normal anatomy and root compliance was revised through the self-expanding property. These left it difficult to determine the factor between root distensibility and sinuses of Valsalva for the improved performance of the valve motion. Newly introduced sinus prosthesis with three separate sinuses and straight commissural pillars resembling the interleaflet triangles and commissures best restores normal root structure. However, the distensibility is restricted because of the noncompliant materials, which leads to abnormal leaflet bending in the systole [31]. Furthermore, some studies show that an aortic root reimplantation in the absence of a reconstruction of the aortic sinuses was not deleterious on valve durability despite abnormal leaflet motion [13, 19, 34]. As concluded from this study, the sinus of Valsalva does not significantly affect the aortic valve's opening motion characteristics, opening area and hemodynamics in a stable distensible aortic root. But closing motion seems to be affected, albeit slightly.

Active engagement in the research and development of new aortic root prosthetic materials with full characteristics of a native distensible root structure is of utmost urgency to encourage valve sparing techniques, to improve valves motion and to enhance valve longevity.

Summary

Objectives---This study was designed to investigate the effects of the sinus of Valsalva on the motion characteristics of the native aortic valve.

Background---Since Leonardo da Vinci first drew and showed the sinus of Valsalva in 1513, field investigation remain limited and somehow controversial. It's hypothesized the aortic sinus may affect the motion characteristics of native aortic valves. We studied these features in a distensible aortic root in the presence or absence of the sinus of Valsalva.

Methods and Results---Nine sections from the porcine aortic root up to ascending-arch transition level were examined in an in-vitro flow simulator. Two groups were investigated: a SINUS group with intact sinus of Valsalva and a NONSINUS group without. Thereby, the distensibility and diameter of the aortic root were preserved. Three distinct phases of aortic valve's motion were evaluated. The valve opening time (VOT), maximum opening area ($AVOA_1$) and opening velocity remained unchanged, while a shortening of the initial slow systolic closing time (ISSCT, $p=0.018$), a decrease of the slow closing displacement (SCD, $p=0.007$) and the rapid closing velocity (RVCV, $p=0.014$) as a prolongation of the valve rapid closing time (RVCT, $p=0.023$) were observed in the NONSINUS group. In addition, hemodynamic parameters were unchanged in the absence of the sinus of Valsalva.

Conclusion---In a stable distensible aortic root, the sinus of Valsalva does not significantly affect the aortic valve's opening characteristics, opening area and hemodynamics. But closing motion seems to be affected albeit slightly.

Keywords: sinus of valsalva ● aortic valve

Zusammenfassung

Ziel dieser Studie war ein Model zu etablieren, um die Auswirkungen der *Sinus valsalvae* auf die Bewegungseigenschaften der nativen Aortenklappen zu untersuchen.

Das Phänomen der *Sinus valsalvae* ist bereits seit der Zeichnung von Leonardo da Vinci (1452-1519) bekannt, jedoch sind die Erkenntnisse bis heute eingeschränkt und weiterhin in irgendeiner Weise umstritten. Es wird die Hypothese aufgestellt, dass die Aortensinus die Bewegungseigenschaften der nativen Aortenklappen beeinträchtigen können. Daher analysierten wir vorab diese Besonderheiten in einer dehnbaren Aortenwurzel in Anwesenheit sowie in Abwesenheit der *Sinus valsalvae*.

Für die Untersuchungen standen neuen Aortenwurzelabschnitte vom Schweineherzen, die bis zum Übergang zwischen Aorta ascendens und Aortenbogen reichen, zur Verfügung. Diese wurden in einem In-vitro-Flusssimulator untersucht. Zwei Gruppen wurden eingeteilt: eine Sinus-Gruppe mit intakten *Sinus valsalvae* und eine Nonsinus-Gruppe ohne *Sinus valsalvae*. Dabei blieben die Dehnbarkeit und der Durchmesser der Aortenwurzel erhalten. Es wurden drei verschiedene Stadien der Aortenklappenbewegungen ausgewertet: Die Klappenöffnungszeit (VOT), die maximale Öffnungsfläche ($AVOA_1$) und die Klappenöffnungsgeschwindigkeit blieben unverändert, während eine zeitliche Verkürzung des anfänglichen langsamen Verschließens (ISSCT, p=0,018), eine Abnahme der Axialverschiebung des langsamen systolischen Verschließens (SCD, p=0,007) und der Geschwindigkeit des schnellen Klappenverschließens (RVCV, p=0,014), sowie eine zeitliche Verlängerung des schnellen Verschließens (RVCT, p=0,023) jeweils in der Nonsinus-Gruppe beobachtet wurden. Außerdem blieben die hämodynamischen Leitparameter trotz der Abwesenheit von *Sinus valsalvae* unverändert.

In der Aortenwurzel mit stabiler Dehnbarkeit beeinträchtigen die *Sinus valsalvae* die Aortenklappenöffnungseigenschaften, die Öffnungsfläche und die Hämodynamik nicht wesentlich. Die Schließbewegungen scheinen aber betroffen zu sein, jedoch geringfügig.

31

References

1. Albes JM, Wahlers T. Valve-sparing root reduction plasty in aortic aneurysm: the "Jena" technique. Ann Thorac Surg. 2003 Mar;75 (3):1031-3.

2. Andreas M, Seebacher G, Reida E, Wiedemann D, Pees C, Rosenhek R, Heinze G, Moritz A, Kocher A, Laufer G. A single-center experience with the ross procedure over 20 years. Ann Thorac Surg. 2014 Jan;97(1):182-8.

3. Apaydin AZ, Posacioglu H, Nalbantgil S, Nart D. Supravalvular aortic stenosis: repair with the Yacoub procedure. J Heart Valve Dis. 2004 Nov; 13(6):921-4.

4. Arjmand Shabestari A, Pourghorban R, Tehrai M, Pouraliakbar H, Faghihi Langroudi T, Bakhshandeh H, Abdi S. Comparison of aortic root dimension changes during cardiac cycle between the patients with and without aortic valve calcification using ECG-gate 64-slice and dual-source 256-slice computed tomography scanners: results of a multicenter study. Int J Cardiovasc Imaging. 2013 Aug;29(6):1391-400.

5. Bechtel JF, Erasmi AW, Misfeld M, Sievers HH. Reconstructive surgery of the aortic valve: the Ross, David and Yacoub procedures. Herz. 2006 Aug; 31(5): 413-22.

6. Beck A, Thubrikar MJ, Robicsek F. Stress analysis of the aortic valve with and without the sinuses of Valsalva. J Heart Valve Dis. 2001 Jan; 10(1):1-11.).

7. Bellhouse BJ, Bellhouse FH. Mechanism of closure of the aortic valve. Nature 1968; 217:86-7.

8. Bottio T, Buratto E, Dal Lin C, Lika A, Tarzia V, Rizzoli G, Gerosa G. Aortic valve hydronynamics: considerations on the absence of sinuses of Valsalva. J Heart Valve Dis. 2012 Nov;21(6):718-23.

9. Charitos EI, Stierle U, Sievers HH, Misfeld M. Valve-sparing aortic root remodeling with partial preservation of the intact native aortic sinuses. Eur J Cardiothorac Surg. 2009 Sep; 36(3):589-91.

10. De Paulis R, De Matteis GM, Nardi P, et al. Opening and closing characteristics of the aortic valve after valve-sparing procedures using a new aortic root conduit. Ann Thorac Surg 2001; 72: 487-94.

11. El-Hamamsy I, Yacoub MH. Repair, replacement, Ross: how I approach the older child with mixed aortic stenosis/aorticinsufficiency. Semin Thorac Cardiovasc Surg Pediatr Card Surg Annu. 2009:133-8.

12. El-Hamamsy I, Zaki M, Stevens LM, Clark LA, Rubens M, Melina G, Yacoub MH.Rate of progression and functional significance of aortic root calcification after homograft versus freestyle aortic root replacement.Circulation. 2009 Sep 15; 120(11 Suppl):S269-75.

13. Erasmi A, Sievers HH, Scharfschwerdt M, Eckel T, Misfeld M. In vitro hydrodynamics, cusp-bending deformation, and root distensibility for different types of aortic valve-sparing operations: remodelling, sinus prosthesis, and reimplantation. J Thorac Cardiovasc Surg. 2005 Oct; 130(4):1044-9.

14. Hagenah J, Scharfschwerdt M, Stender B, Ott S, Friedl R, Sievers HH, Schlaefer A. A setup for ultrasound based assessment of the aortic root geometry. Biomed Tech (Berl).2013; 58 (Suppl.1)© 2013 by Walter de Gruyter •Berlin•Boston.

15. Hanke T, Charitos EI, Stierle U, Robinson D, Gorski A, Sievers HH, Misfeld M. Factors associated with the development of taortic valve regurgitation over time after two different techniques of valve-sparing aortic root surgery. J Thorac Cardiovasc Surg. 2009 Feb; 137 (2): 314-9.; Sievers HH. Ross procedure. HSR Proc Intensive Care Cardiovasc Anesth. 2012; 4(2): 119-23.

16. Katayama S, Umetani N, Sugiura S, Hisada T. The sinus of Valsalva relieves abnormal stress on aortic valve leaflets by facilitating smooth closure. J Thorac Cardiovasc Surg. 2008 Dec; 136(6):1528-35, 1535.e1.

17. Kollar AC, Lick SD, Conti VR. Integrating resuspension with remodeling: early results with a new valve-sparing aortic root reconstruction technique. J Heart Valve Dis. 2008 Jan; 17(1):74-9; discussion 79-80.

18. Lansac E, Lim HS, Shomura Y, Lim KH, Rice NT, Goetz W, Acar C, Duran CM. A four-dimensional study of the aortic root dynamics. Eur J Cardiothorac Surg. 2002 Oct;22(4):497-503.

19. Leyh RG, Schmidtke C, Sievers HH, et al. Opening and closing characteristics of the aortic valve after different types of valve-preserving surgery. Circulation 1999; 100: 2153-60.

20. López-Mínguez JR, Climent V, Yen-Ho S, González-Fernández R, Nogales-Asensio JM, Sánchez-Quintana D. Strutural features of the sinus of valsalva and the proximal portion of the coronary arteries: their relevance to retrograde aortocoronary dissection. Rev Esp Cardio (Engl ed). 2006; 59(7):696-702.

21. Luciani GB, Viscardi F, Pilati M, Prioli AM, Faggian G, Mazzucco A. The Ross-Yacoub procedure for aneurysmal autograft roots: a strategy to preserve autologous pulmonary valves. J Thorac Cardiovasc Surg. 2010 Mar; 139(3):536-42.

22. Maselli D, Weltert L, Scaffa R, De Paulis R. How to achieve an aortic root remodelling by performing an aortic root reimplantation. Eur J Cardiothorac Surg. 2012 Nov; 42(5): e136-7.

23. Patel ND, Arnaoutakis GJ, George TJ, Allen JG, Alejo DE, Dietz HC, Cameron DE, Vricella LA. Valve-sparing aortic root replacement in children: intermediate-term results. Interact Cardiovasc Thorac Surg. 2011 Mar; 12(3):415-9.

24. Peacock JA. An in vitro study of the onset of turbulence in the sinus of Valsalva. Circ Res. 1990 Aug; 67(2): 448-60.

25. Peskin CS, Wolfe AW. The aortic sinus vortex. Fed Proc. 1978 Dec; 37(14):2784-92.

26. Pisani G, Scaffa R, Ieropoli O, Dell'Amico EM, Maselli D, Morbiducci U, De Paulis R. Role of the sinuses of Valsalva on the opening of the aortic valve. J Thorac Cardiovasc Surg. 2013 Apr;145(4):999-1003.

27. Rahnavardi M,Yan TD, Bannon PG, Wilson MK. Aortic valve-sparing operations in aortic root aneurysms: remodeling or reimplantation? Interact Cardiovasc Thorac Surg. 2011 Aug; 13(2):189-97.

28. Robicsek F. Leonardo da Vinci and the sinuses of Valsalva. Ann Thorac Surg. 1991 Aug; 52(2):328-35.

29. Scharfschwerdt M, Misfeld M, Sievers HH. The influence of a nonlinear resistance element upon in vitro aortic pressure tracings and aortic valve motions. ASAIO J. 2004 Sep-Oct; 50(5):498-502.

30. Scharfschwerdt M, Richter A, Boehmer K, Repenning D, Sievers, HH. Improved hydrodynamics of a new aortic cannula with a novel tip design. Perfusion. 2004 May; 19(3):193-7.

31. Schmidtke C, Sievers HH, Frydrychowicz A, et al. First clinical results with the new sinus prosthesis used for valve-sparing aortic root replacement. Eur J Cardiothorac Surg 2012.

32. Shrestha M, Khaladj N, Baraki H, Al Ahmad A, Koigeldiyev N, Pichlmaier M, Haverich A, Hagl C. Aortic root reoperation: a technical challenge. J Heart Valve Dis. 2010 Mar; 19(2):177-81.

33. Sievers HH. Ross procedure. HSR Proc Intensive Care Cardiovasc Anesth. 2012; 4(2): 119-23.

34. Sievers HH. Status of aortic valve reconstruction and Ross operation in aortic valve diseases. Herz. 2002 Aug; 27(5):435-44.

35. Sievers HH, Schmidtke C. A classification system for the bicuspid aortic valve from 304 surgical specimens. J Thorac Cardiovasc Surg 2007; 133:1226-33.

36. Soncini M, Votta E, Zinicchino S, Burrone V, Mangini A, Lemma M, Antona C, Redaelli A. Aortic root performance after valve sparing procedure: a comparative finite element analysis. Med Eng Phys. 2009 Mar; 31(2): 234-43.

37. Subramanian S, Leontyev S, Borger MA, Trommer C, Misfeld M, Mohr FW. Valve-sparing root reconstruction does not compromise survival in acute type A aortic dissection. Ann Thorac Surg. 2012 Oct; 94(4):1230-4.

38. Thubrikar MJ. The Aortic Valve. 1st ed. Boca Raton, Florida, US: CRC Press, Inc., 1981.

39. Torii R, El-Hamamsy I, Donya M, Babu-Narayan SV, Ibrahim M, Kilner PJ, Mohiaddin RH, Xu XY, Yacoub MH. Integrated morphologic and functional assessment of the aortic root after different tissue valve root replacement procedures. J Thorac Cardiovasc Surg. 2012 Jun; 143(6):1422-8.

40. Van Steenhoven AA, van Dongen MEH. Model studies of the closing behaviour of the aortic valve. J. Fluid Mech. (1979), vol. 90, part 1, pp. 21-32.

41.   Wittlinger T, Aybek T, Moritz A, Kleine P, Martens S, Wimmer-Greinecker G. Indication, technique, and results of aortic valve and ascending aorta reconstruction. Herz. 2006 Oct; 31(7):676-84. German

List of figures

List of tables

Measured Values

	Sinus Valsalva	t_1 (VOT) (sec)	t_2 (sec) *	t_2-t_1 (ISSCT) (sec) *	t_3 (sec)	t_3-t_2 (RVCT) (sec) *
No1	Yes	0.070	0.346	0.276	0.408	0.062
	No	0.072	0.292	0.220	0.398	0.106
No2	Yes	0.102	0.346	0.244	0.442	0.096
	No	0.098	0.340	0.242	0.440	0.100
No3	Yes	0.068	0.336	0.268	0.402	0.066
	No	0.066	0.320	0.254	0.404	0.084
No4	Yes	0.074	0.340	0.266	0.408	0.068
	No	0.074	0.326	0.252	0.438	0.112
No5	Yes	0.070	0.324	0.254	0.416	0.092
	no	0.074	0.278	0.204	0.376	0.098
No6	yes	0.082	0.348	0.266	0.404	0.056
	no	0.082	0.344	0.262	0.420	0.076
No7	yes	0.072	0.344	0.272	0.422	0.078
	no	0.072	0.322	0.250	0.402	0.080
No8	yes	0.062	0.338	0.276	0.394	0.056
	no	0.054	0.304	0.250	0.390	0.086
No9	yes	0.066	0.316	0.250	0.388	0.072
	no	0.060	0.320	0.260	0.384	0.064

Tab. 9 : Time registration for the hemodynamic motion of aortic valve in vitro HL-simulator in details.

	Sinus Valsava	AVOA$_1$ (cm^2)	AVOA$_1$/t$_1$ (cm^2•s^{-1})	AVOA$_2$	ΔAVOA$_{1-2}$ (cm^2) *	SCD (%)
No1	yes	3.481	49.73	2.474	1.007	28.93
	no	3.055	42.43	2.481	0.574	18.79
No2[#]	yes	3.511	34.42	2.640	0.871	24.81
	no	3.324	33.92	2.339	0.985	29.63
No3	yes	3.651	53.69	2.571	1.080	29.58
	no	3.298	49.97	2.498	0.800	24.26
No4	yes	3.674	49.65	2.723	0.951	25.88
	no	3.271	44.20	2.682	0.589	18.01
No5	yes	3.292	47.03	2.444	0.848	25.76
	no	2.987	40.37	2.380	0.607	20.32
No6	yes	3.684	44.93	2.013	1.671	45.36
	no	3.374	41.15	1.971	1.403	41.58
No7	yes	3.578	49.69	2.282	1.296	36.22
	no	3.020	41.94	2.321	0.699	23.15
No 8	yes	2.529	40.79	1.455	1.074	42.47
	no	2.096	38.82	1.487	0.609	29.06
No 9	yes	3.079	46.65	1.642	1.437	46.67
	no	2.581	43.02	1.527	1.054	40.84

Tab. 10 : Effective orifice areas recorded and analyzed in course of the physiological opening and closing motion of the aortic valve in details.

	Sinus Valsalva	Pieces $_{t2-t1}$ *	ISSCV=ΔAVOA$_{1-2}$/pie$_{t2-t1}$ (cm^2/pic) *	ISSCV=ΔAVOA$_{1-2}$/(t$_2$-t$_1$) (cm^2/decisec) *
No1	yes	138	0.007297	0.364855
	no	110	0.005218	0.260909
No2	yes	122	0.007139	0.356967
	no	121	0.008140	0.407025
No3	yes	134	0.008060	0.402985
	no	127	0.006299	0.314961
No4	yes	133	0.007150	0.357519
	no	126	0.004675	0.233730
No5	yes	127	0.006677	0.333858
	no	102	0.005951	0.297549
No6	yes	133	0.012564	0.628195
	no	131	0.010710	0.535496
No7	yes	136	0.009529	0.476471
	no	125	0.005592	0.279600
No8	yes	138	0.007783	0.389130
	no	125	0.004872	0.243600
No9	yes	125	0.011496	0.574800
	no	130	0.008108	0.405385

Tab. 11 : Detailed analysis of initial slow systolic valve closing phase in sense of initial slow closing velocity with different aspects.

	Sinus Valsalva	t_3-t_2 (RVCT) (sec) *	$AVOA_2(cm^2)$	RVCV=$AVOA_2$/RVCT (cm^2/sec)
No1	Yes	0.062	2.474	39.90323
	No	0.106	2.481	23.40566
No2	Yes	0.096	2.640	27.50000
	No	0.100	2.339	23.39000
No3	Yes	0.066	2.571	38.95455
	No	0.084	2.498	29.73810
No4	Yes	0.068	2.723	40.04412
	No	0.112	2.682	23.94643
No5	Yes	0.092	2.444	26.56522
	no	0.098	2.380	24.28571
No6	yes	0.056	2.013	35.94643
	no	0.076	1.971	25.93421
No7	yes	0.078	2.282	29.25641
	no	0.080	2.321	29.01250
No8	yes	0.056	1.455	25.98214
	no	0.086	1.487	17.29070
No9	yes	0.072	1.642	22.80556
	no	0.064	1.527	23.85938

Tab. 12 : Detailed analysis of the rapid valve closing motion with presentation of the rapid valve closing velocities (RVCV) and rapid valve closing time

Acknowledgements

My deepest gratitude goes first and foremost to Professor Dr.med. Hans-Hinrich Sievers, the principal of clinic of cardiac and thoracic vascular surgery, my supervisor, for his excellent guidance, caring, patience, and providing me with an excellent atmosphere for doing research. I am deeply grateful of his inspiring suggestions in the completion of this thesis.

High tribute shall be paid to Dr. Michael Scharfschwerdt, whose professional knowledge triggers my love for this thesis. Without his consistent and illuminating instruction, this thesis could not have reached its present form.

Finally I like to express my gratitude to my beloved parents who have been always supporting me and encouraging me with their best wishes.

Curriculum vitae

Junfeng Yan Dr.

Stiller Winkel 4

23562 Lübeck

Mobil: 0176 / 70 43 13 74

e-mail: yxingqiao@gmail.com

Personal Data

Birth name:	06. September 1976
Birthplace:	Liaoning
Nationality:	Chinese
Civil status:	married
Mother:	Suju Zhuang, pharmacist
Father:	Bo Yan, electronic engineer

Work Experience

03.11 – dato	resident in the clinic of cardiac and thoracic vascular surgery of the university zu Lübeck
06.99 – 08.01	orthodontist in dental clinic Dalian, China
10.01 – 10.02	continued education of orthodontics in university of Washington-Health Sciences school of dentistry, Seattle, USA

Education

10.06 – 01.11	Ruprecht-Karls University Heidelberg, Germany Diplom in Human Medicine
10.02 – 08.06	Johns Hopkins University School of Medicine, USA

44

	Ph.D. in Neuroscience
08.94 – 08.99	Medical University Dalian, China
	Master in Dentistry
08.88 – 08.94	First Key Middle School Liaoyang, China
	High-school diploma
08.82 – 07.88	Elementary School Liaoyang, China

Lübeck, Germany, June 8th 2014